

Direct calculation of the S matrix in coordinate space

Helmut Kröger and Rodolfo J. Slobodrian

Département de Physique, Université Laval, Québec, Canada G1K 7P4

Gerald L. Payne

Department of Physics and Astronomy, University of Iowa, Iowa City, Iowa 52242

(Received 30 July 1987)

We test the strong approximation of the Møller wave operator scheme in coordinate space for N-N scattering using the local Malfliet-Tjon IV potential. Using spline expansion functions we obtain a finite-dimensional Hamiltonian matrix with a band structure which brings about a considerable numerical advantage when diagonalizing it. We compute the S matrix and find satisfactory agreement with a standard solution. We also compute the violation of energy conservation.

I. INTRODUCTION

In recent years a new branch of physics has grown between experimental and theoretical physics, the so-called computational physics. In order to make a physical problem amenable to a numerical solution on the computer sometimes requires or often strongly suggests a new mathematical formulation, the best known example of this kind being the lattice formulation of field theory.

In this sense we want to discuss here an alternative formulation for the numerical computation of nonrelativistic few-body scattering. If a physical system is described by the Schrödinger equation governed by a time-independent Hamiltonian H , its time evolution is given by $U(t) = \exp(iHt)$. This quantity is of central importance in the computation of a scattering process. If H is self-adjoint, then $U(t)$ is unitary and analytic. These are two very important properties which have far-reaching implications on a numerical computation. However, in the standard time-independent formulation of stationary scattering theory, these two properties are used explicitly nowhere. Hence we want to advocate an approach here which makes use of these properties. In the strong approximation of the Møller wave operator approach, one computes $U(t)$ in the following way (see, e.g., Ref. 1): One approximates the Hamiltonian H by a finite-dimensional Hamiltonian $H(N)$ and approximates $U(t) = \exp(iHt)$ by $U(N, t) = \exp[iH(N)t]$. The last expression is suitable for the numerical calculation on a modern computer. Nineteen different methods of computing the exponential of a matrix have been compared by Moler and Van Loan.² In our case—where $H(N)$ is self-adjoint—it has been suggested to diagonalize $H(N)$,

$$H(N) = \sum_{k=1}^n |\phi_{(k)}\rangle E_{(k)} \langle \phi_{(k)}|, \quad (1.1)$$

and to compute $U(N, t)$ in the eigenrepresentation of $H(N)$,

$$U(N, t) = \sum_{k=1}^n |\phi_{(k)}\rangle \exp(iE_{(k)}t) \langle \phi_{(k)}|. \quad (1.2)$$

It should be noted that the diagonalization of a matrix is a task well suited for a vector computer. While the time evolution is not a physical observable, however, the S matrix is. The S matrix contains the information on the time evolution plus the boundary conditions. The S matrix is usually expressed to incorporate the boundary conditions in the time-dependent language, i.e., via the time evolution of the asymptotic Hamiltonians. Considering the case that all interactions are of short range and the asymptotic Hamiltonian H^0 is the same for the asymptotic incoming state as for the asymptotic outgoing state, the asymptotic time evolution is $U^0(t) = \exp(iH^0t)$ and the S matrix is given by

$$S = \lim_{t \rightarrow \infty} U^0(t)U(-2t)U^0(t). \quad (1.3)$$

In order to compute the S matrix numerically, it is consistent to approximate also the asymptotic Hamiltonian H^0 by a finite-dimensional one, $H^0(N)$, and the time evolution by $U^0(N, t) = \exp[iH^0(N)t]$. In a numerical computation we replace the time limit in Eq. (1.3) by a large but finite time parameter T , i.e., our approximate S matrix reads

$$S(N, T) = U^0(N, T)U(N, -2T)U^0(N, T). \quad (1.4)$$

It has been demonstrated in a number of cases that this approach works, if the dynamics are described by the Schrödinger equation: for the two-body system with different short range interactions,^{1,3} also when the long range Coulomb force is involved (which requires a slight modification of the asymptotic time evolution).¹ It has also been applied in the three-body case to the reaction $p(d, pp)n$.⁴ Moreover, it has been shown to work for a number of field theoretical models such as the nonlinear Schrödinger model,⁵ the ϕ^4 theory in $1+1$ dimensions,⁶ and the massive Thirring model.⁷

In a numerical calculation for a system with a large number of degrees of freedom (which is already the case in the three-nucleon system), due to the large size of the Hamilton matrices, one soon reaches the limit of the computer, i.e., the limit of storage location and comput-

ing time (note that the latter increases with the cube of the dimension of the matrix). Hence it is of crucial importance to reduce the effective dimensions of the problem. The same kind of problem occurring in the coordinate space formulation of lattice field theory has been successfully solved by the Monte Carlo method. In our approach to compute the S matrix and in order to reduce the effective dimension there are several possibilities:

(i) One possibility is to use a separable interaction. This allows one to rewrite the eigenvalue equation and leads to an algebraic reduction for the same reason the effective dimension of a Lippman-Schwinger or Faddeev-type integral equation is reduced.⁸ This kind of reduction technique has been employed and proven useful in the nonlinear Schrödinger model,⁵ ϕ^4 theory,⁶ and the massive Thirring model.⁷

(ii) Another possibility is to go into the light cone frame and discretize light cone momentum and energy. In $1+1$ dimensions the light cone momentum is positive, which puts drastic constraints on the effective dimension of the discretized system. This technique has been applied to compute the spectrum of the Yukawa model⁹ and the massive Schwinger model.¹⁰

(iii) Another powerful way is the application of the Monte Carlo method, which has been demonstrated so successfully in lattice field theory. One way to apply the Monte Carlo method to scattering problems has been suggested in Ref. 11.

The intention of this paper is to discuss a further alternative to reduce the effective dimension of the system. The basic idea is to use a representation in which the Hamiltonian is not a full but a sparse matrix, in particular, a band matrix. This is a matrix that has nonzero entries only in the main diagonal and in a few neighbor diagonals. It is well known that the diagonalization of a band matrix is much easier than that of a full matrix. The idea to represent a Hamiltonian in the form of a band matrix has been extensively used for the solution of bound state problems in nuclear, atomic, and molecular physics as well as many other physical and engineering problems.¹²⁻¹⁴ In this paper we want to advocate the idea to apply it to a scattering problem. As has been shown by the Los Alamos-Iowa group,^{12,15} a convenient and useful way to obtain a band matrix Hamiltonian is to use a spline representation in coordinate space. As will be shown in the next section, the free Hamiltonian has a band structure in a coordinate space spline representation. To ensure that the full Hamiltonian also has a band structure, it is sufficient that the interaction be local. Hence the aim of this paper is to show that the S matrix can be obtained from our time-dependent approximation scheme (1.4), where the finite-dimensional approximate Hamiltonians have a band structure originating from a coordinate space spline representation. We consider a two-nucleon system interacting via a local short range potential of Malfliet-Tjon type. We compare the S matrix obtained from our scheme with a reference S matrix obtained in a standard way. The investigations presented here are considered as a prerequisite paving the way for an application of the method to the three-

nucleon system with realistic local interactions. In Sec. II we present the formalism, in Sec. III we present and discuss the results, and in Sec. IV we give some conclusions.

II. FORMALISM

Let us consider a two-body system in the center of mass system. Let us assume that the two particles are spinless, each of mass m , and they interact via a local central potential $V(r)$. Then the Hamiltonian $H = H^0 + V$ reads, in coordinate representation,

$$\langle \mathbf{r}' | H | \mathbf{r} \rangle = \delta(\mathbf{r}' - \mathbf{r}) \left[\frac{-\hbar^2}{2\mu} \Delta + V(r) \right], \quad (2.1)$$

where $\mu = m/2$ is the reduced mass. For the mathematically interested reader, we want to mention that H^0 is an essentially self-adjoint operator on $S(\mathbb{R}_3)$, where $S(\mathbb{R}_3)$ is the linear manifold of rapidly decreasing functions over \mathbb{R}_3 .¹⁶ Because the potential is rotationally invariant, H can be expressed in an invariant subspace of angular momentum l ,

$$\langle r'lm | H | rlm \rangle = \frac{\delta(r' - r)}{r^2} \left[-\frac{\hbar^2}{2\mu} \left[\frac{d^2}{dr^2} + \frac{2}{r} \frac{d}{dr} - \frac{l(l+1)}{r^2} \right] + V(r) \right]. \quad (2.2)$$

We use the standard $L_2(\mathbb{R}_3)$ scalar product

$$\langle \psi | \phi \rangle = \int_0^\infty dr r^2 \psi^*(r) \phi(r), \quad (2.3)$$

which for the reduced wave functions $\psi(r) = u(r)/r$ and $\phi(r) = v(r)/r$ reads

$$\langle u | v \rangle_R = \int_0^\infty dr u^*(r) v(r). \quad (2.4a)$$

In the rest of this paper we work with the reduced wave functions and for convenience of notation we drop the index "R" and the angular momentum quantum numbers l and m ,

$$\langle u | v \rangle = \langle u | v \rangle_R. \quad (2.4b)$$

Thus a matrix element of the Hamiltonian reads

$$\langle u | H | v \rangle = \int_0^\infty dr u^*(r) \left[-\frac{\hbar^2}{2\mu} \left[\frac{d^2}{dr^2} - \frac{l(l+1)}{r^2} \right] + V(r) \right] v(r). \quad (2.5)$$

Now we are ready to introduce a finite-dimensional set of basis functions, which will eventually lead to the finite-dimensional full and asymptotic Hamiltonians, introduced in Sec. I. We will use, in particular, cubic Hermitian splines (for the general theory and application of splines, see Refs. 17 and 18). We have chosen spline

functions, because they have the following important features. Firstly, they are localized functions, i.e., there is only a finite domain, where the function values are nonzero. On that domain, they are defined as polynomials, i.e., they are smooth functions. As a consequence they are a powerful tool in approximating smooth functions (they are far superior to any set of orthogonal polynomials). Secondly, they can be chosen such that each spline function has an overlap with at most N other spline functions. In our case we will have $N=5$. As a consequence, the matrix elements of the Hamiltonian taken between spline functions will have a band structure. We take the definition of the cubic Hermitian splines given in Ref. 15. Let the interval $[0, R_{\max}]$ be partitioned into I subintervals $0=r_0 < r_1 < \dots < r_{I-1} < r_I = R_{\max}$. There are $2I+2$ spline functions:

$$\phi_\alpha(r) = \left[\frac{r-r_{\alpha-1}}{r_\alpha-r_{\alpha-1}} \right]^2 \left[3-2 \left[\frac{r-r_{\alpha-1}}{r_\alpha-r_{\alpha-1}} \right] \right], \quad r_{\alpha-1} \leq r < r_\alpha \quad (2.6a)$$

$$\phi_\alpha(r) = \left[\frac{r_{\alpha+1}-r}{r_{\alpha+1}-r_\alpha} \right]^2 \left[3-2 \left[\frac{r_{\alpha+1}-r}{r_{\alpha+1}-r_\alpha} \right] \right], \quad r_\alpha \leq r < r_{\alpha+1} \quad (2.6b)$$

$$\xi_\alpha(r) = \left[\frac{r-r_{\alpha-1}}{r_\alpha-r_{\alpha-1}} \right]^2 (r-r_\alpha), \quad r_{\alpha-1} \leq r < r_\alpha \quad (2.6c)$$

$$\xi_\alpha(r) = \left[\frac{r_{\alpha+1}-r}{r_{\alpha+1}-r_\alpha} \right]^2 (r-r_\alpha), \quad r_\alpha \leq r < r_{\alpha+1} \quad (2.6d)$$

One example for the case $I=5$ is given in Figs. 1 and 2.

Physics imposes the following constraints on the wave functions. The reduced radial wave function $u(r)$ has to have the asymptotic property

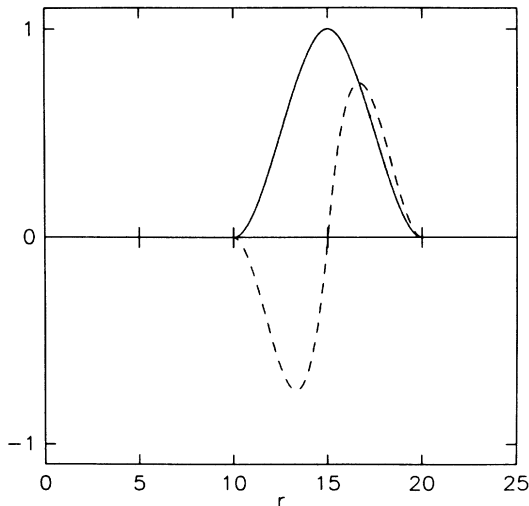


FIG. 1. The cubic Hermite spline functions ϕ_3 (solid line) and ξ_3 (dashed line) for $I=5$, $R_{\max}=25$.

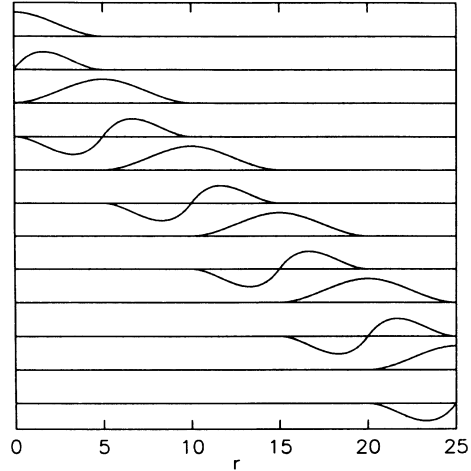


FIG. 2. Cubic Hermite splines for $I=5$, $R_{\max}=25$.

$$u(r) \underset{r \rightarrow \infty}{\sim} 0. \quad (2.7a)$$

The property that the wave function is in the domain of the Hamiltonian implies the asymptotic property

$$u(r) \underset{r \rightarrow 0}{\sim} 0. \quad (2.7b)$$

Because we want to approximate the wave function by spline functions, we impose the conditions (2.7a) and (2.7b) as constraints on our set of spline functions, i.e., we drop those splines which are nonzero at $r=0$ and $r=R_{\max}$ (see Fig. 2). Thus we are left with $N=2I$ spline functions, which we renumber from 1 to N and which then form our working basis of expansion functions $\{s_\alpha\}$, $\alpha=1, 2, \dots, N$.

It should be noted that the functions s_α are neither orthogonal nor normalized to unity with respect to the scalar product given by Eq. (2.4b). The matrix σ , defined as

$$\sigma_{\alpha\beta} = \langle s_\alpha | s_\beta \rangle, \quad (2.8)$$

is a real, symmetric, positive matrix, which is invertible. The matrix σ has a band structure; σ^{-1} , however, does not. One can construct an orthonormal set of basis functions

$$|e_\alpha\rangle = \sum_{\beta=1}^N (\sigma^{-1/2})_{\alpha\beta} |s_\beta\rangle \quad (2.9)$$

and an orthogonal projector $P(N)$ onto the set $\{s_\alpha\}$, $\alpha=1, 2, \dots, N$,

$$P(N) = \sum_{\alpha,\beta=1}^N |s_\alpha\rangle (\sigma^{-1})_{\alpha\beta} \langle s_\beta|. \quad (2.10)$$

From the projector we obtain the finite-dimensional Hamiltonians

$$H(N) = P(N)HP(N), \quad (2.11a)$$

$$H^0(N) = P(N)H^0P(N). \quad (2.11b)$$

In principle, Eqs. (2.10) and (2.11) define our finite-dimensional Hamiltonians, which can be diagonalized [Eq. (1.1)], yielding the time evolution [Eq. (1.2)] and the S matrix [Eq. (1.4)]. However, from the numerical point of view, this procedure would not be the optimum one because it involves the computation of the matrix σ^{-1} , which does not have a band structure. Hence we would give up our desired goal to operate with sparse matrices of band structure. Fortunately, it is possible to proceed while avoiding σ^{-1} completely. Let us consider, e.g., the eigenvalue equation

$$H(N) |\phi_{(k)}\rangle = E_{(k)} |\phi_{(k)}\rangle, \quad k = 1, \dots, N. \quad (2.12)$$

In the following we denote by (s) that we operate in the spline representation. That is, we define

$$H_{\alpha\beta}(s) = \langle s_\alpha | H | s_\beta \rangle, \quad (2.13)$$

$$\phi_{(k)\alpha}(s) = \langle s_\alpha | \phi_{(k)} \rangle. \quad (2.14)$$

The eigenstate can be expressed as

$$|\phi_{(k)}\rangle = \sum_{\alpha=1}^N |s_\alpha\rangle \psi_{(k)\alpha}, \quad (2.15)$$

where $\psi_{(k)\alpha}$ is the α th component of a vector, which is the solution of the generalized eigenvalue equation

$$[H(s) - E_{(k)}\sigma] \psi_{(k)} = 0. \quad (2.16)$$

One should note that all matrices appearing in this equation have a band structure. This is the equation we solve numerically on the computer. After diagonalizing the Hamiltonian $H(N)$, we can express the time evolution [Eq. (1.2)] as

$$U(N, T) = \sum_{\alpha, \beta, k=1}^N |s_\alpha\rangle \psi_{(k)\alpha} \exp(iE_{(k)}T) \psi_{(k)\beta} \langle s_\beta|. \quad (2.17)$$

Before proceeding to the S matrix, let us introduce the asymptotic wave packets. We assume that the asymptotic wave packets, given in coordinate space, are eigenstates of total angular momentum l and 3-component m , i.e.,

$$\phi^{\text{as}}(\mathbf{r}) = \phi^{\text{as}}(r) Y_{lm}(\hat{\mathbf{r}}). \quad (2.18)$$

Again we introduce the reduced wave function $u^{\text{as}}(r)$ via

$$\phi^{\text{as}}(\mathbf{r}) = \frac{u^{\text{as}}(r)}{r}. \quad (2.19)$$

Using the notation of Eq. (2.4), we write the asymptotic state as $|u^{\text{as}}\rangle$. Then, we can express the S matrix, given by Eq. (1.4), as

$$\begin{aligned} \langle u'^{\text{as}} | S(N, T) | u^{\text{as}} \rangle = & \sum_{\substack{i, j, k, \\ \alpha, \beta, \gamma, \delta, \epsilon, \xi=1}} u'^{\text{as}}_{\alpha}(s) \psi_{(i)\alpha}^0 \exp(iE_{(i)}^0 T) \psi_{(i)\beta}^0 \sigma_{\beta\gamma} \psi_{(j)\gamma} \exp(-i2E_{(j)} T) \psi_{(j)\delta} \sigma_{\delta\epsilon} \\ & \times \psi_{(k)\epsilon}^0 \exp(iE_{(k)}^0 T) \psi_{(k)\xi}^0 u^{\text{as}}_{\xi}(s), \end{aligned} \quad (2.20)$$

where

$$u_{\alpha}^{\text{as}}(s) = \langle s_\alpha | u^{\text{as}} \rangle. \quad (2.21)$$

The relative error of the approximation $S(N, T)$ of the physical S matrix S is measured by

$$\Delta_S(N, T) = \left| \frac{\langle u'^{\text{as}} | S(N, T) - S | u^{\text{as}} \rangle}{\langle u'^{\text{as}} | S | u^{\text{as}} \rangle} \right|. \quad (2.22)$$

We will introduce two functions, $\Delta_{<>}(N, T)$ and $\Delta_0(N, T)$, both of which will measure the violation of energy conservation of the approximate S matrix. Based on the intertwining relations

$$\Omega^{(\pm)} H^0 = H \Omega^{(\pm)} \quad (2.23)$$

and the commutation property of the S matrix

$$[S, H^0] = 0, \quad (2.24)$$

Eq. (2.23) implies

$$\langle \Omega^{(\pm)} u'^{\text{as}} | H | \Omega^{(\pm)} u^{\text{as}} \rangle = \langle u'^{\text{as}} | H^0 | u^{\text{as}} \rangle. \quad (2.25)$$

Denoting

$$\Omega(N, T) = U(N, T) U^0(N, -T), \quad (2.26)$$

we define

$$\Delta_{<>}(N, T) = \left| \frac{\langle \Omega(N, T) u'^{\text{as}} | H(N) | \Omega(N, T) u^{\text{as}} \rangle - \langle u'^{\text{as}} | H^0(N) | u^{\text{as}} \rangle}{\langle u'^{\text{as}} | H^0(N) | u^{\text{as}} \rangle} \right|. \quad (2.27)$$

Because

$$[U(N, T), H(N)] = 0, \quad (2.28)$$

$\Delta_{< >}(N, T)$ can also be expressed as

$$\Delta_{< >} = \left| \frac{\langle u'^{\text{as}} | U^0(N, T) H^{\text{int}}(N) U^0(N, -T) | u^{\text{as}} \rangle}{\langle u'^{\text{as}} | H^0(N) | u^{\text{as}} \rangle} \right|. \quad (2.29)$$

Equation (2.24) implies

$$\langle u'^{\text{as}} | H^0 S (H^0)^{-1} | u^{\text{as}} \rangle = \langle u'^{\text{as}} | S | u^{\text{as}} \rangle \quad (2.30)$$

for those asymptotic states $|u^{\text{as}}\rangle$, for which $(H^0)^{-1} |u^{\text{as}}\rangle$ exists. We define

$$\Delta_0(N, T) = \left| \frac{\langle u'^{\text{as}} | H^0(N) S(N, T) [H^0(N)]^{-1} - S(N, T) | u^{\text{as}} \rangle}{\langle u'^{\text{as}} | S(N, T) | u^{\text{as}} \rangle} \right|. \quad (2.31)$$

III. NUMERICAL RESULTS

We have used the following interaction: the triplet part of the local Malfliet-Tjon IV potential,^{19,20} given by

$$V(r) = \lambda \frac{e^{-ar}}{r}, \quad (3.1a)$$

$$a = 0.633 \text{ fm}^{-1}, \quad (3.1b)$$

$$\lambda = -65.120 \text{ MeV fm}^{-1}. \quad (3.1c)$$

We have chosen the following wave packet: an s -wave state given in momentum space by

$$\phi^{\text{as}}(\mathbf{k}) = \phi^{\text{as}}(k) Y_{00}(\mathbf{k}), \quad (3.2a)$$

$$\phi^{\text{as}}(k) = \frac{v^{\text{as}}(k)}{k}, \quad (3.2b)$$

$$v^{\text{as}}(k) = \kappa 2 \sin^2 \left[\pi \frac{k_{\text{up}} - k}{k_{\text{up}} - k_{\text{low}}} \right] \times \theta(k_{\text{up}} - k) \theta(k - k_{\text{low}}), \quad (3.2c)$$

$$\kappa = \left[\frac{3}{2} (k_{\text{up}} - k_{\text{low}}) \right]^{-1/2}. \quad (3.2d)$$

The constant κ has been chosen such that $\phi^{\text{as}}(\mathbf{k})$ is nor-

malized to unity in $L_2(\mathbb{R}_3)$. The function $v^{\text{as}}(k)$ yields a bell-shaped wave packet with a maximum at $k_{\text{max}} = \frac{1}{2}(k_{\text{up}} + k_{\text{low}})$ and a half-width $k_{\text{wid}} = \frac{1}{2}(k_{\text{up}} - k_{\text{low}})$. We have chosen the wave packet parameters $k_{\text{low}} = 1.0 \text{ fm}^{-1}$ and $k_{\text{up}} = 2.0 \text{ fm}^{-1}$. This corresponds to the energies $E_{\text{low}} = 41.47 \text{ MeV}$ and $E_{\text{up}} = 165.9 \text{ MeV}$. The expectation value of the asymptotic Hamiltonian in this asymptotic state is $\langle E \rangle = 94.13 \text{ MeV}$. We have chosen the asymptotic incoming and outgoing wave packets to be identical. In order to obtain the reduced wave packet $u^{\text{as}}(r)$ in coordinate space, we compute from $\phi^{\text{as}}(\mathbf{k})$ its Fourier transformation, separate the angular dependence, and form the reduced wave packet by dividing by r . One has the relation

$$u^{\text{as}}(r) = \left[\frac{2}{\pi} \right]^{1/2} \frac{1}{r} \int_0^\infty dx \sin(x) v^{\text{as}} \left[\frac{x}{r} \right]. \quad (3.3)$$

In Fig. 3 we have plotted the s -wave phase shifts in this energy region. The phase shifts have been obtained by solving the Schrödinger equation plus boundary conditions in coordinate space in a standard way and are considered as our reference values for our approximative solution. The phase shifts display a smooth behavior over the energy range covered by the wave packet. We have used for our finite-dimensional approximation

TABLE I. The relative error of the norm $\|u^{\text{as}}\|$ and the relative error of the expectation value $\langle u^{\text{as}} | H^0 | u^{\text{as}} \rangle$ in the spline approximation as a function of the length R_{max} of the coordinate space interval and the number N of spline functions. $E - n$ denotes 10^{-n} .

R_{max} (fm)	10	20	30	N 40	50	60	70
10.0	0.172 306 0.167 937E - 2	0.948 200E - 2 0.913 304E - 2	0.327 000E - 2 0.103 184E - 1				
20.0	0.349 864 0.117 371E - 1	0.168 134 0.732 339E - 2	0.205 560E - 1 0.119 613E - 2	0.692 400E - 2 0.577 883E - 3	0.293 000E - 2 0.290 003E - 3		
30.0	0.123 727E + 1 0.880 100	0.215 228 0.197 627	0.168 098 0.734 676E - 2	0.316 510E - 1 0.156 793E - 2	0.138 310E - 1 0.932 686E - 3	0.689 700E - 2 0.573 633E - 3	0.379 800E - 2 0.359 052E - 3

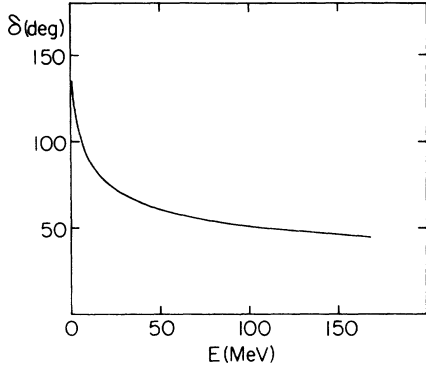


FIG. 3. The s -wave phase shifts of the Malfliet-Tjon IV potential given by Eq. (3.1).

scheme intervals in coordinate space characterized by $R_{\max} = 10, 20,$ and 30 fm. We have always considered an equidistant partition of that interval. The dimension N of the basis has been varied between 10 and 70. The quality of the spline approximation of the asymptotic wave packet has been tested by computing the norm of the wave packet and the expectation value of the asymptotic Hamiltonian both in the spline representation and as the reference value from a continuous integral. The results are shown in Table I. One observes convergence towards the reference value when increasing R_{\max} and N . Note that for large R_{\max} and N , the relative error is basically determined by N/R_{\max} , which is a measure for the nodal density in coordinate space. This ratio also determines an upper limit of the derivative in the spline representation, and hence determines an upper limit of the kinetic energy. Because the potential chosen is always negative, this also determines an upper limit $E_{\max}(N, R_{\max})$ of the total energy. One observes, qualitatively,

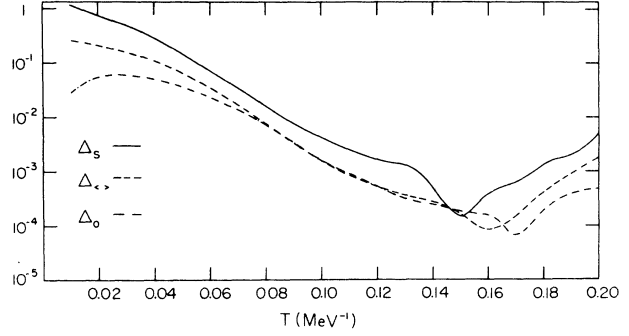


FIG. 5. Same as Fig. 4, but $R_{\max} = 20$ fm, $N = 50$.

$$E_{\max}(N, R_{\max}) = \alpha(N/R_{\max})^2, \quad (3.4a)$$

$$\alpha = 435 \text{ MeV fm}^2. \quad (3.4b)$$

In order to obtain a reasonably converged result for the expectation value of the asymptotic Hamiltonian, one has to make sure that $E_{\max}(N, R_{\max})$ is larger than the largest energy contributing to the wave packet. We have chosen a wave packet which has a low and a high energy cutoff, E_{low} and E_{up} , respectively, and fulfills the latter condition in all cases investigated. Another parameter, which plays a role, when studying the approximation of the scattering wave function, is the averaged spectral density of the energy. The total number of eigenvalues is identical to the dimension N of the Hamiltonian. Hence the averaged spectral density is $N/E_{\max}(N, R_{\max})$. The scattering wave function, in general, has contributions from all momenta up to infinity. One expects that the errors for the S matrix in the spline representation will depend on both the spectral density and E_{\max} .

Now let us discuss the results for the S -matrix calculations. The results are presented in Figs. 4–6 and Tables II–IV. We display the S -matrix elements, given by Eq. (2.20), and, moreover, $\Delta_S(N, T)$, defined by Eq. (2.22),

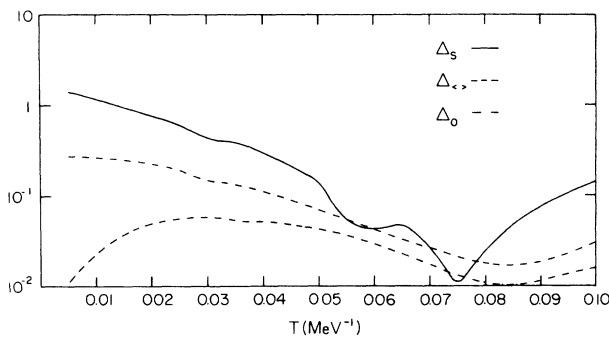


FIG. 4. Dependence of the relative error $\Delta_S(N, T)$ of the S -matrix element, given by Eq. (2.22), and the error functions $\Delta_{<>}(N, T)$ and $\Delta_0(N, T)$, given Eqs. (2.27) and (2.31), respectively, on the scattering time T . The wave packet is bell-shaped, given by Eqs. (3.2) and (3.3) and characterized by the parameters $k_{\text{low}} = 1.0 \text{ fm}^{-1}$ and $k_{\text{up}} = 2.0 \text{ fm}^{-1}$. The interval covered by the spline functions is $[0, R_{\max}]$ with $R_{\max} = 10$ fm. The number of spline functions is $N = 30$.

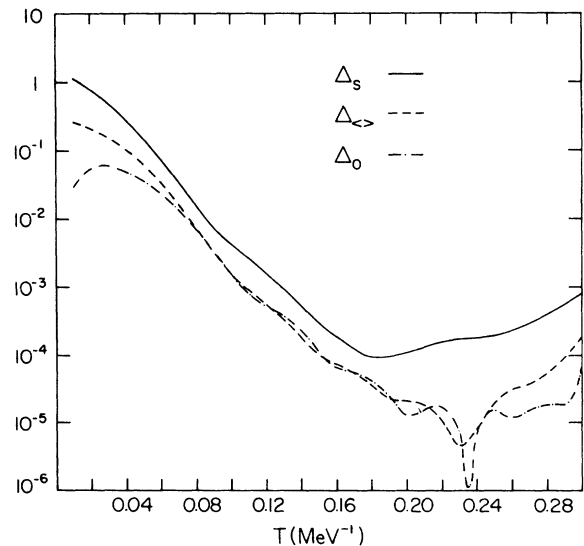


FIG. 6. Same as Fig. 4, but $R_{\max} = 30$ fm, $N = 70$.

TABLE II. Dependence of the S -matrix element $\langle u^{\text{as}} | S(N, T) | u^{\text{as}} \rangle$, given by Eq. (2.20), its relative error $\Delta_S(N, T)$, given by Eq. (2.22), and the error functions $\Delta_{< >}(N, T)$ and $\Delta_0(N, T)$, given by Eqs. (2.27) and (2.31), respectively, on the number N of spline expansion functions and the scattering time T . In each box the top entry corresponds to $\text{Re}[S(N, T)]$, the second to $\text{Im}[S(N, T)]$, the third to $\Delta_S(N, T)$, the fourth to $\Delta_{< >}(N, T)$, and the bottom to $\Delta_0(N, T)$. The wave packet is bell shaped, given by Eqs. (3.2) and (3.3), characterized by the parameters $k_{\text{low}} = 1.0 \text{ fm}^{-1}$ and $k_{\text{up}} = 2.0 \text{ fm}^{-1}$. The reference value of the S matrix is $S = -0.242 510 + 0.965 621i$ and $|S| = 0.995 607$. The interval covered by the spline functions is $[0, R_{\text{max}}]$ with $R_{\text{max}} = 10 \text{ fm}$. $E - n$ denotes 10^{-n} .

$T \text{ (MeV)}^{-1}$	N		
	10	20	30
0.01	0.764 321	0.774 601	0.774 923
	0.403 437	0.397 117	0.396 563
	0.115 315E + 1	0.116 520E + 1	0.116 576E + 1
	0.280 612	0.267 591	0.266 587
	0.214 470E - 1	0.229 903E - 1	0.234 374E - 1
0.02	0.400 357	0.427 069	0.428 330
	0.614 078	0.606 880	0.605 882
	0.732 707	0.759 625	0.761 208
	0.230 913	0.221 390	0.223 019
	0.463 446E - 1	0.489 501E - 1	0.495 308E - 1
0.03	0.160 261	0.202 323	0.150 185
	0.740 657	0.734 941	0.773 939
	0.461 338	0.501 088	0.436 979
	0.173 509	0.165 912	0.149 779
	0.599 966E - 1	0.565 378E - 1	0.582 705E - 1
0.04	-0.243 634E - 1	0.313 197E - 1	0.334 162E - 1
	0.856 414	0.859 298	0.857 277
	0.243 955	0.293 746	0.296 434
	0.110 288	0.112 349	0.110 008
	0.643 287E - 1	0.551 096E - 1	0.525 574E - 1
0.05	-0.163 041	-0.109 091	-0.106 382
	0.923 912	0.926 940	0.925 777
	0.897 494E - 1	0.138 913	0.141 839
	0.626 370E - 1	0.685 714E - 1	0.704 810E - 1
	0.486 195E - 1	0.442 257E - 1	0.428 138E - 1
0.06	-0.227 571	-0.175 178	-0.174 391
	0.942 626	0.953 457	0.953 449
	0.274 215E - 1	0.684 269E - 1	0.691 979E - 1
	0.370 830E - 1	0.413 072E - 1	0.421 214E - 1
	0.323 279E - 1	0.288 550E - 1	0.290 042E - 1
0.07	-0.270 385	-0.216 465	-0.216 410
	0.942 293	0.958 017	0.958 337
	0.359 221E - 1	0.271 323E - 1	0.270 973E - 1
	0.221 739E - 1	0.252 662E - 1	0.256 449E - 1
	0.183 015E - 1	0.171 474E - 1	0.170 106E - 1
0.08	-0.313 821	-0.260 473	-0.260 726
	0.929 652	0.948 817	0.948 811
	0.798 688E - 1	0.245 976E - 1	0.247 870E - 1
	0.147 234E - 1	0.176 565E - 1	0.178 053E - 1
	0.112 178E - 1	0.103 360E - 1	0.103 811E - 1
0.09	-0.348 439	-0.305 128	-0.305 426
	0.899 493	0.921 782	0.921 350
	0.124 875	0.764 386E - 1	0.769 307E - 1
	0.158 528E - 1	0.183 348E - 1	0.183 031E - 1
	0.138 852E - 1	0.119 898E - 1	0.114 522E - 1
0.10	-0.375 207	-0.350 682	-0.348 212
	0.835 927	0.861 264	0.867 758
	0.185 550	0.150 304	0.144 048
	0.344 086E - 1	0.293 722E - 1	0.298 925E - 1
	0.203 128E - 1	0.161 225E - 1	0.159 435E - 1

TABLE III. Same as Table II, but $R_{\max} = 20$ fm.

T (MeV) $^{-1}$	10	20	N 30	40	50
0.02	0.597 275	0.406 106	0.429 437	0.430 272	0.430 395
	0.613 960	0.608 153	0.604 045	0.603 703	0.603 610
	0.910 441	0.740 598	0.763 053	0.763 950	0.764 102
	0.312 132	0.229 485	0.220 084	0.223 281	0.223 126
	0.418 811E - 1	0.627 481E - 1	0.565 811E - 1	0.572 464E - 1	0.572 226E - 1
0.04	0.266 173	-0.105 119E - 1	0.343 433E - 1	0.351 124E - 1	0.351 921E - 1
	0.831 124	0.850 817	0.855 007	0.854 694	0.854 747
	0.526 163	0.258 849	0.298 132	0.298 963	0.299 017
	0.532 134	0.110 909	0.111 491	0.112 032	0.112 067
	0.669 070E - 1	0.533 345 - 1	0.499 238 - 1	0.498 381E - 1	0.497 833E - 1
0.06	-0.369 779E - 1	-0.227 379	-0.173 779	-0.173 809	-0.173 727
	0.877 824	0.933 364	0.943 459	0.943 558	0.943 580
	0.223 498	0.356 294E - 1	0.722 156E - 1	0.721 567E - 1	0.722 281E - 1
	0.134 245	0.335 642E - 1	0.366 408E - 1	0.367 287E - 1	0.366 774E - 1
	0.864 597E - 1	0.260 533E - 1	0.249 271E - 1	0.249 049E - 1	0.248 408E - 1
0.08	-0.187 232	-0.279 843	-0.226 432	-0.226 596	-0.226 550
	0.876 128	0.950 576	0.963 783	-0.964 000	0.964 087
	0.105 188	0.402 505E - 1	0.161 872E - 1	0.159 963E - 1	0.160 335E - 1
	0.735 844E - 1	0.590 579E - 2	0.766 712E - 1	0.768 801E - 2	0.765 461E - 1
	0.338 558E - 1	0.755 679E - 2	0.753 792E - 2	0.743 018E - 2	0.752 748E - 2
0.10	-0.279 576	-0.289 694	-0.238 419	-0.238 486	-0.238 357
	-0.853 908	0.952 682	0.964 801	0.964 909	0.964 968
	0.117 701	0.489 259E - 1	0.417 237E - 2	0.408 650E - 2	0.420 402E - 2
	0.475 267E - 1	0.129 420E - 2	0.160 680E - 2	0.155 648E - 2	0.155 584E - 2
	0.275 967E - 1	0.142 804E - 2	0.164 455E - 2	0.159 981E - 2	0.161 251E - 2
0.12	-0.326 851	-0.291 293	-0.241 071	-0.241 038	-0.240 896
	0.793 525	0.953 177	0.965 044	0.965 111	0.965 163
	0.191 651	0.503 451E - 1	0.155 037E - 2	0.155 784E - 2	0.167 772E - 2
	0.347 328E - 1	0.107 943E - 2	0.637 958E - 3	0.549 156E - 3	0.546 895E - 3
	0.327 970E - 1	0.447 785E - 3	0.647 952E - 3	0.549 518E - 3	0.542 468E - 3
0.14	-0.308 807	0.293 475	-0.242 405	-0.242 167	-0.242 011
	0.749 665	0.953 204	0.965 275	0.965 465	0.965 516
	0.225 903	0.524 558E - 1	0.361 581E - 3	0.376 808E - 3	0.509 927E - 3
	0.339 752E - 1	0.880 983E - 3	0.303 396E - 3	0.282 461E - 3	0.284 852E - 3
	0.302 142E - 1	0.394 500E - 3	0.417 871E - 3	0.258 153E - 3	0.257 587E - 3
0.16	-0.274 128	-0.295 655	-0.243 246	-0.242 983	-0.242 824
	0.753 105	0.953 007	0.965 022	0.965 305	0.965 368
	0.214 855	0.546 214E - 1	0.948 945E - 3	0.568 845E - 3	0.403 243E - 3
	0.378 597E - 1	0.219 824E - 1	0.131 610E - 3	0.852 265E - 4	0.887 598E - 4
	0.300 135E - 1	0.321 488E - 3	0.191 490E - 3	0.147 513E - 3	0.153 165E - 3
0.18	-0.247 857	-0.296 331	-0.243 666	-0.243 435	-0.243 278
	0.762 541	0.952 430	0.964 516	0.964 869	0.964 876
	0.203 150	0.554 139E - 1	0.159 917E - 2	0.119 211E - 2	0.106 997E - 2
	0.332 260E - 1	0.330 867E - 3	0.460 297E - 3	0.439 385E - 3	0.428 378E - 3
	0.351 341E - 1	0.292 115E - 3	0.277 961E - 3	0.256 927E - 3	0.249 352E - 3
0.20	-0.231 567	-0.298 531	-0.247 324	-0.244 245	-0.244 078
	0.765 016	0.948 724	0.962 540	0.962 997	0.962 874
	0.200 903	0.585 137E - 1	0.571 551E - 2	0.422 783E - 2	0.494 099E - 2
	0.256 515E - 1	0.191 502E - 2	0.176 014E - 2	0.175 320E - 2	0.174 200E - 2
	0.256 431E - 1	0.458 813E - 3	0.474 980E - 3	0.486 494E - 3	0.495 980E - 3

TABLE IV. Same as Table II, but $R_{\max} = 30$ fm.

T (MeV) ⁻¹	N			
	10	30	50	70
0.02	0.878 366	0.406 158	0.430 073	0.430 430
	0.328 471	0.608 100	0.603 813	0.603 579
	0.128 931E + 1	0.740 669	0.763 723	0.764 148
	0.279 485E + 1	0.229 467	0.224 546	0.223 132
	0.258 318	0.621 698E - 1	0.574 569E - 1	0.569 138E - 1
0.04	0.560 670	-0.104 171E - 1	0.347 906E - 1	0.352 369E - 1
	0.581 884	0.850 733	0.854 689	0.854 705
	0.890 141	0.258 971	0.298 666	0.299 074
	0.209 428E + 1	0.110 895	0.111 946	0.112 056
	0.502 209	0.535 979E - 1	0.501 183E - 1	0.499 520E - 1
0.06	0.157 147	-0.227 236	-0.173 788	-0.173 645
	0.715 061	0.933 412	0.943 424	0.943 535
	0.471 705	0.356 470E - 1	0.722 187E - 1	0.723 199E - 1
	0.143 740E - 1	0.335 323E - 1	0.366 457E - 1	0.367 088E - 1
	0.591 923	0.262 613E - 1	0.250 064E - 1	0.250 011E - 1
0.08	-0.223 916	-0.279 707	-0.226 554	-0.226 509
	0.727 052	0.950 503	0.963 824	0.963 988
	0.239 292	0.401 518E - 1	0.160 568E - 1	0.160 841E - 1
	0.959 420	0.593 723E - 2	0.766 191E - 2	0.764 079E - 2
	0.582 100	0.750 349E - 2	0.746 074E - 2	0.745 926E - 2
0.10	-0.521 107	-0.289 553	-0.238 455	-0.238 305
	0.152 992	0.952 587	0.964 770	0.964 882
	0.418 751	0.488 152E - 1	0.414 333E - 2	0.426 944E - 2
	0.640 462	0.132 303E - 2	0.154 697E - 2	0.153 116E - 2
	0.549 293	0.129 642E - 2	0.156 840E - 2	0.153 137E - 2
0.12	-0.722 455	-0.291 254	-0.241 078	-0.240 895
	0.540 587	0.953 220	0.965 041	0.965 148
	0.641 093	0.502 967E - 1	0.168 240E - 2	0.168 248E - 2
	0.432 703	0.985 021E - 3	0.600 762E - 3	0.594 953E - 3
	0.512 043	0.497 483E - 3	0.586 410E - 3	0.584 769E - 3
0.14	-0.843 776	-0.292 451	-0.242 181	-0.241 989
	0.424 823	0.953 426	0.965 373	0.965 479
	0.808 692	0.514 083E - 1	0.412 001E - 3	0.540 004E - 3
	0.297 523	0.687 001E - 3	0.183 047E - 3	0.181 840E - 3
	0.473 644	0.201 232E - 3	0.215 176E - 3	0.232 820E - 3
0.16	-0.908 345	-0.294 000	-0.242 586	-0.242 367
	0.334 162	0.952 614	0.965 390	0.965 496
	0.917 647	0.531 074E - 1	0.243 181E - 3	0.189 931E - 3
	0.208 408	0.412 290E - 3	0.758 351E - 4	0.770 444E - 4
	0.435 442	0.251 427E - 3	0.456 087E - 4	0.687 576E - 4
0.18	-0.937 004	-0.294 823	-0.242 799	-0.242 524
	0.264 318	0.951 698	0.965 387	0.965 513
	0.986 989	0.541 340E - 1	0.371 856E - 3	0.965 512E - 4
	0.148 180	0.145 183E - 3	0.530 635E - 4	0.364 016E - 4
	0.397 973	0.204 753E - 3	0.717 984E - 4	0.447 481E - 4
0.20	-0.945 456	-0.295 104	-0.242 879	-0.242 589
	0.215 800	0.951 155	0.965 388	0.965 544
	0.102 779E + 1	0.545 471E - 1	0.436 405E - 3	0.110 317E - 3
	0.106 088	0.726 549E - 4	0.295 642E - 4	0.222 282E - 4
	0.360 602	0.364 995E - 4	0.150 462E - 4	0.133 274E - 4
0.22	-0.944 315	-0.295 177	-0.242 949	-0.242 654
	0.184 084	0.950 945	0.965 383	0.965 547
	0.105 039E + 1	0.546 735E - 1	0.499 364E - 3	0.161 901E - 3
	0.758 340E - 1	0.150 613E - 3	0.115 352E - 4	0.107 778E - 4
	0.321 901	0.698 876E - 4	0.206 771E - 4	0.176 540E - 4

TABLE IV. (Continued).

T (MeV) ⁻¹	N			
	10	30	50	70
0.24	-0.939 845	-0.295 471	-0.242 969	-0.242 673
	0.164 755	-0.950 910	0.965 375	0.965 539
	0.106 191E + 1	0.549 661E - 1	0.520 765E - 3	0.182 463E - 3
	0.539 624E - 1	0.330 942E - 3	0.987 837E - 5	0.826 228E - 5
	0.281 068	0.848 833E - 4	0.951 697E - 5	0.784 466E - 5
0.26	-0.934 897	-0.296 115	-0.243 024	-0.242 725
	0.154 006	0.951 253	0.965 351	0.965 516
	0.106 682E + 1	0.554 971E - 1	0.580 599E - 3	0.239 269E - 3
	0.384 845E - 1	0.443 875E - 3	0.350 356E - 4	0.331 241E - 4
	0.239 265	0.665 120E - 4	0.124 247E - 4	0.123 571E -
0.28	-0.930 288	-0.297 835	-0.243 196	-0.242 890
	0.148 612	0.951 545	0.965 263	0.965 431
	0.106 796E + 1	0.570 875E - 1	0.773 795E - 3	0.424 852E - 3
	0.279 056E - 1	0.358 512E - 3	0.563 175E - 4	0.533 050E - 4
	0.201 535	0.858 534E - 4	0.188 567E - 4	0.184 425E - 4
0.30	-0.926 276	-0.299 764	-0.243 490	-0.243 175
	0.146 127	0.951 014	0.964 969	0.965 155
	0.106 728E + 1	0.590 879E - 1	0.117 707E - 2	0.812 022E - 3
	0.207 857E - 1	0.308 805E - 3	0.190 053E - 3	0.195 900E - 3
	0.170 076	0.703 412E - 2	0.781 140E - 4	0.704 360E - 4

which determines the relative error of the approximate S matrix [to be precise, we have displayed the numerator of the right-hand side (rhs) of Eq. (2.22), because the absolute value of the denominator differs from 1 only in the third digit]. Moreover, we have displayed $\Delta_{< >}(N, T)$ and $\Delta_0(N, T)$, given by Eqs. (2.27) and (2.31), respectively, which both measure the violation of energy conservation. The general observation made is the following: For each value of T , the approximate S matrix $S(N, T)$ converges as a function of N . For each value of N , $S(N, T)$ is a periodic function of T . The period is a function of N and increases with N . In practice, the following question arises: For a given N , which is the best value of T , such that $\Delta_S(N, T)$ becomes minimal? The same kinds of properties of the approximate S matrix have been observed when applying the technique in momentum space.¹¹ In Ref. 1 an answer to this question has been given. Roughly speaking, the error in the S matrix is minimal as a function of T , when the violation of energy conservation is minimal. Thus, in cases where the exact S matrix is unknown, one would determine the best value of T from the minimum of $\Delta_{< >}(N, T)$ or $\Delta_0(N, T)$. Note that both are functions which do not require the knowledge of the exact S matrix or scattering states, but only the approximate ones.

An approximate value of T for the minimal error can be obtained by considering the motion of the wave packet in coordinate space. Choosing a particular value of R corresponds to placing the wave packet in a box whose size is R . The time evolution operator moves the wave packet both in time and space, and the distance moved must be less than the size of the box. Also, the value of T must be large enough so that the wave packet is well

outside the region where the potential is nonzero. For large values of T only the tail of the wave packet is in the region of the potential and as T becomes larger the overlap of the wave packet with the potential decreases. Thus for large values of T one can obtain a good approximation to the S matrix. However, as mentioned above the value of T is limited by the size of the box. An approximate limit on the value of T can be found by using the time for the free wave packet to move across the box. Using the relationship $p = \hbar k = mv$, one finds $T = mR / (\hbar^2 k)$. For $k = 1.5 \text{ fm}^{-1}$ and $R = 10 \text{ fm}$, the value of T is 0.161 MeV^{-1} . The actual value of T will be smaller than this because of the finite size of the wave packet and the spreading of the wave packet in time. From Fig. 4 one can see that the error is a minimum for $T = 0.075 \text{ MeV}^{-1}$. Comparing Figs. 4–6 we find that the optimal value of T is a linear function of R .

Comparing the absolute magnitude in the relative errors of the norm of the asymptotic states and the expectation value of the asymptotic Hamiltonian, given in Table I, with the relative error of the S matrix, given in Table II–IV, it seems that in some cases the S matrix is more accurate than the norm of the asymptotic state and the expectation value of the asymptotic Hamiltonian. This is due to the fact that we have renormalized to unity the spline expansion of the asymptotic state before computing the S matrix.

IV. CONCLUSIONS

We have demonstrated for the case of a two-nucleon system that a finite-dimensional spline approximation of a nonrelativistic Hamiltonian is suitable not only for the

purpose of calculating the bound state spectrum,^{12–14} but also for the computation of the S matrix. We find a fairly rapid convergence of the approximate S matrix toward the reference solution. The important feature of the spline representation, applied in the case of a local potential, is that it yields a Hamiltonian matrix of the band structure. What are the implications for an eventual application of this method for the computation of the S matrix of a three-nucleon system, using the Reid or Paris or Bonn potential? Also, in a three-nucleon sys-

tem interacting via local potentials one would obtain a Hamiltonian of the band structure. Currently, people have treated—on modern supercomputers—band matrices of dimensions of the order of 10^6 . Thus we are cautiously optimistic that three-nucleon scattering calculations based on this method using realistic interactions are now feasible.

This work was supported by the Natural Sciences and Engineering Research Council of Canada.

-
- ¹M. Batinić, Ž. Bajzer, and H. Kröger, *Phys. Rev. C* **33**, 1187 (1986).
²C. Moler and C. Van Loan, *SIAM Rev.* **20**, 801 (1978).
³H. Kröger and R. J. Slobodrian, *Phys. Rev. C* **30**, 1390 (1984).
⁴H. Kröger, A. M. Nachabe, and R. J. Slobodrian, *Phys. Rev. C* **33**, 1208 (1986).
⁵R. Girard and H. Kröger, *Phys. Rev. D* **34**, 1824 (1986).
⁶H. Kröger, R. Girard, and G. Dufour, *Phys. Rev. D* **35**, 3944 (1987).
⁷R. Girard and H. Kröger, *Z. Phys. C* (in press).
⁸H. Kröger, *Phys. Rev. C* **31**, 1118 (1985).
⁹H. C. Pauli and S. J. Brodsky, *Phys. Rev. D* **32**, 1993 (1985); **32**, 2001 (1985).
¹⁰T. Eller, H. C. Pauli, and S. J. Brodsky, *Phys. Rev. D* **35**, 1493 (1987).
¹¹H. Kröger, *Phys. Rev. A* **35**, 4525 (1987).
¹²C. R. Chen, G. L. Payne, J. L. Friar, and B. F. Gibson, *Phys. Rev. Lett.* **55**, 374 (1985).

- ¹³W. K. Ford and F. S. Levin, *Phys. Rev. A* **29**, 43 (1984).
¹⁴M. Friedman, Y. Rosenfeld, A. Rabinovitch, R. Thieberger, *J. Comput. Phys.* **26**, 169 (1978).
¹⁵G. L. Payne, Configuration Space Faddeev Calculations: Numerical Methods, Lecture presented at the 8th Autumn School on Models and Methods in Few-Body Physics, Lisboa, Portugal, 1986.
¹⁶W. O. Amrein, J. M. Jauch, and K. B. Sinha, *Scattering Theory in Quantum Mechanics*, Vol. 16 of *Lecture Notes and Supplements in Physics* (Benjamin, Reading, Mass., 1977), Proposition 3.9, p. 117.
¹⁷P. M. Prenter, *Splines and Variational Methods* (Wiley, New York, 1975).
¹⁸C. de Boor, *A Practical Guide to Splines* (Springer-Verlag, Berlin, 1978).
¹⁹R. A. Malfiet and J. A. Tjon, *Nucl. Phys.* **A127**, 161 (1969).
²⁰J. L. Friar, B. F. Gibson, and G. L. Payne, *Z. Phys. A* **301**, 309 (1981).